

CALIBRATION OF AN ANECHOIC CHAMBER FOR MEASUREMENT OF A MULTI-CHANNEL ANTENNA

T. Sheret

Centre for Wireless Research
University of Bedfordshire
United Kingdom
Email: tamara.sheret@beds.ac.uk

B. Allen

Centre for Wireless Research
University of Bedfordshire
United Kingdom
Email: ben.allen@beds.ac.uk

Abstract—Anechoic chambers are structures which simulate testing in free space and are used to measure the radiation pattern of an antenna. This paper presents a methodology to measure the radiation properties and hence determine the gain of a multi-channel antenna in an anechoic chamber. This gives an unique extension to current practice that is only suitable for a single channel antenna. The process to measure the loss through an anechoic chamber measurement system and the gain measurement of a multi-channel antenna are presented and a measurement procedure is recommended.

I. INTRODUCTION

Anechoic chambers are rooms designed to absorb the reflections of electromagnetic radiation [1] and to minimise interfering energy disturbances from external spurious sources [2]. Such chambers are used to measure the performance of the Antenna Under Test (AUT), in particular gain and pattern characteristics.

Typically, the chamber wall construction is a Faraday cage which prevents external signals entering the chamber and interfering with measurements. This also prevents test signals escaping from the chamber, which may interfere with external devices and be a potential health risk [3]. The interior of an anechoic chamber is lined with Radar-Absorbent Material (RAM) [4] with construction and lay-out to provide Radio Frequency (RF) signal absorption across the required frequency band. The measurement system requires a transmit signal source of RF energy in the correct frequency range and a receive system that is capable of measuring the signal received by the AUT, such as a Programmable Network Analyser (PNA). To hold and move the AUT, a positioning system is installed in the chamber which has the required number of axes to complete the required AUT testing.

RAM is used on the internal walls of anechoic chambers as it attenuates the unwanted RF signals. The internal lay-out of the RAM in anechoic chambers is designed to create a ‘quiet zone’ around the antenna under test (AUT). The RAM lay-out to create the

required quiet zone can be simulated in commercially available electromagnetic simulation packages such as CST Microwave studio or ANSYS HFSS, or by more traditional ray tracing techniques [5]. The outcome of this design process will be a RAM lay-out which results in a size and level of the quiet zone as required by the type of testing and the AUT.

A positioning system is required in the chamber to hold and to move the AUT. The positioning system has the required number of degrees-of-freedom to complete the desired measurements on the AUT [6]. These positioning systems are manufactured from metal and therefore have to be covered in RAM to avoid producing spurious reflections.

If a low power measurement is to be taken it is possible to use the PNA as the transmit power source and the receive measurement system. The RF transmit signal produced in the PNA can be routed via coaxial cables to a standard gain transmit horn. The signal is then received by the AUT and the receive signal routed to the PNA for measurement via coaxial cables. If a higher power source is needed then additional amplifiers may be required in the RF path before the transmit Standard Gain Horn (SGH). If this does not produce sufficient power the transmit power source can be changed to a solid state power amplifier or a travelling-wave tube with additional hardware to ensure phase stabilisation between the transmit power source and the receiving PNA.

Anechoic chambers are used for convenience over an open air range. Taking measurements in an anechoic chamber is logistically easier than an outdoor range as the site is smaller, contained within an existing building with amenities and its functionality is independent of weather. In addition it is easier to measure the AUT phase with respect to the reference signal as the distances involved are smaller. The chamber also helps to minimise the health and safety impact of working with high power RF radiation under the Occupational Exposure to Non-Ionizing Radiation guidelines from

the National Radiological Protection Board [3] as transmissions are contained.

However, because anechoic chambers simulate an outdoor range and can only minimise spurious RF reflections, the performance of the chamber has to be properly assessed. Range effects such as spurious reflections can be identified by measuring the AUT at different rotational orientations, to see if the reflection features in the pattern rotate with the antenna (antenna effect) or stay in the same location (range effect). Ideally, testing will always be made on an outdoor range and in the anechoic chamber, so the differences for each AUT are known.

There are alternatives to anechoic chambers which can be used to measure AUT's. To reduce construction costs it is possible to use a semi-anechoic chamber, where only the walls and ceiling have RAM installed [7], however the issues raised are still applicable for this kind of chamber. Open air ranges, which minimise spurious reflections, can be used but these are large, expensive and difficult to work on. Slant ranges [8] can be used, but tend to also be outside and suffer the same drawbacks as open air ranges. Rather than using a simple transmit and receive anechoic chamber, a compact range [8] could be used which helps to minimise the size of the anechoic chamber. However, this is a more complicated construction and has detrimental effects on cross polar measurements. If power measurements alone are required, a 'ram dump' could be used, which is a RAM lined metal box which absorbs incident RF radiation. For certain antennas it is possible to measure the near field of an antenna and transpose this into the far field [9]. This is a complicated process and measurements need to be taken with great care. Devices such as the EMSCAN RFxpert can make this process more robust to get real-time near-field measurements [10].

To measure an antenna, the path losses and phase changes in the measurement system must be determined and their effects calibrated out. To measure this calibration in an anechoic chamber, a SGH is measured on the positioner in the chamber. These results can be used to measure the loss and the phase change through the chamber and therefore provide input for chamber calibration.

A multi-channel antenna is an antenna with more than one input and output channel, for example an array or a monopulse antenna. It is important that each channel of the AUT is measured without a magnitude or phase imbalance being introduced between channels due to differences or movement in measurement hardware. The acceptable level of error between measurements in the magnitude and phase will be defined by the requirements of the individual AUT. Traditional chamber calibration methods are designed to cope with only one channel, therefore a calibration method needs

to be defined to cope with a multi-channel AUT. In this case the magnitude and phase of each channel of the antenna have to be measured and therefore the magnitude and phase of each channels RF path needs to be measured for the calibration and applied to the relevant channel.

This paper describes the hardware set up in a full anechoic chamber, which uses a PNA as the RF signal and measurement unit. It is novel because it describes the procedure to measure multi-channel antenna systems. However, the process of measurement and calibration would also be applicable to other types of ranges, semi-anechoic chambers, slant and outdoor ranges.

II. ANECHOIC CHAMBER AND POSITIONING SYSTEM

Figure 1 shows the schematic for the full anechoic chamber designed for antenna testing [5]. The site is divided into three sections: the transmit room; the chamber; and the control room, all of which are screened rooms. The control room contains the control system for the range and is fully automated via PC control by use of custom written MATLAB scripts. The PNA produces the transmitted signal, routed to the transmit horn via a co-axial cable, and analyses the received signal via a co-axial cable attached to the AUT. In the Anechoic Chamber the positioner carries the AUT and can orientate it to measure plots in Azimuth and Elevation and produce full antenna patterns. The positioning system is a roll over elevation over azimuth three axis positioner [6]. The metal structure of the positioner is covered in RAM to prevent stray RF reflections. The transmit room allows the safe transmitting of the amplified PNA signal which can then be received by the AUT on the positioner without exposing any users of the range to the radiation. It has a transmit positioner, which holds the transmit horn, and provides the main lighting for the chamber.

Additional hardware has to be introduced to allow the measurement of multiple channels; this can be of the form of a multiplexer behind the antenna and a single channel PNA, or multiple cables coming from the back of the AUT into a multi-channel PNA. The multiplexer is formed of a series of terminated RF switches and is PC controlled. The choice of hardware design is dependent on the measurement requirements on the AUT and will be the subject of a further paper. This paper will discuss a chamber which uses a multiplexer behind the antenna and a single channel PNA.

III. SIZE OF AN ANECHOIC CHAMBER

An anechoic chamber provides an environment to simulate free-space testing, the internal size of the chamber is of paramount importance. To ensure there are no undue interference from the walls of the chamber, the

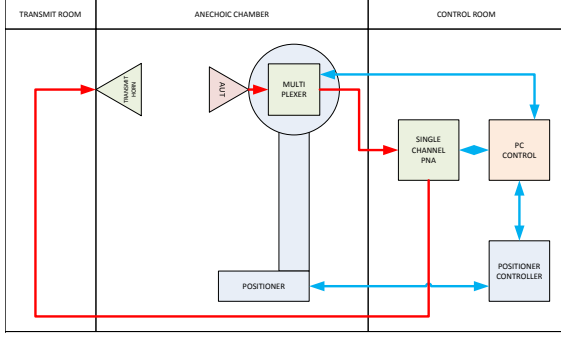


Fig. 1. Schematic representation of anechoic chamber used for multi-channel antenna measurement with a multiplexer and a single channel PNA.

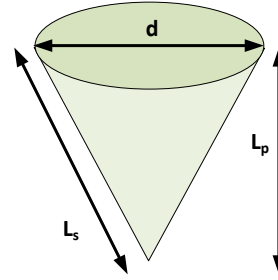


Fig. 2. Showing the dimensions of the conical horn to be simulated.

distance to the structure forming the ceiling, floor and side walls from the AUT should be greater than the Raleigh distance and the distance to the transmit wall should be greater than twice the Raleigh distance [11]. The Raleigh distance defines the far-field of an antenna based on its diameter (D (m)) and the wavelength of operation (λ (m)) and is shown in equation 1. If the chamber used to measure the performance of an AUT is too small the measurements will be taken in the near-field and the results disturbed, thus the true far-field antenna performance is not measured. However, if the chamber is too large there is no degradation to the measurement, just an increase in manufacture, running costs and real estate requirements. In some measurement techniques it is possible to correct for near-field effects, these will not be discussed in this paper.

$$Raleigh\ Distance = \frac{2 D^2}{\lambda} \quad (1)$$

For example, from equation 1, an AUT with diameter 150 mm working at a frequency of 15 GHz has a Raleigh Distance of 2.25 m. Therefore the minimum chamber dimensions are 5 m wide by 5 m + distance from the front of the positioner to the back wall of the chamber by 5 m high.

A. Simulation of size of anechoic chamber

To show the effect of measuring an AUT in a chamber of the incorrect dimensions a HFSS simulation was set up of a conical horn, as shown in figure 2. The simulation is split along two symmetry planes using perfect E and H boundaries to reduce the electrical size of the model, as shown in figure 3. This has an aperture diameter (d (m)) of 150mm, with optimal perpendicular length (L_P (m)) of 367mm to give maximum gain and minimum reflection, as calculated from equation 2 [12] at 15 GHz. L_P is calculated from the slant length of the side of the horn (L_S (m)) using $\frac{d}{2}$ and Pythagorass theorem.

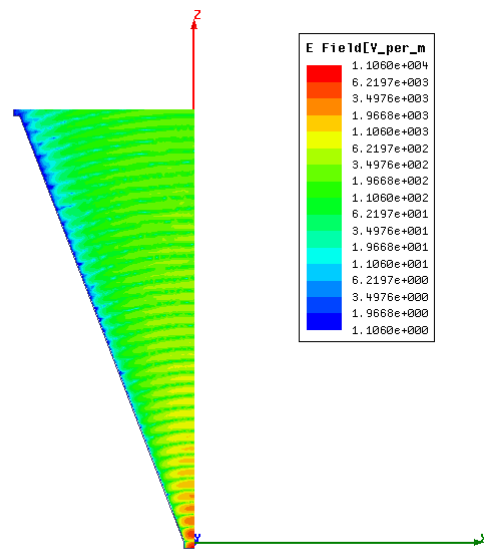
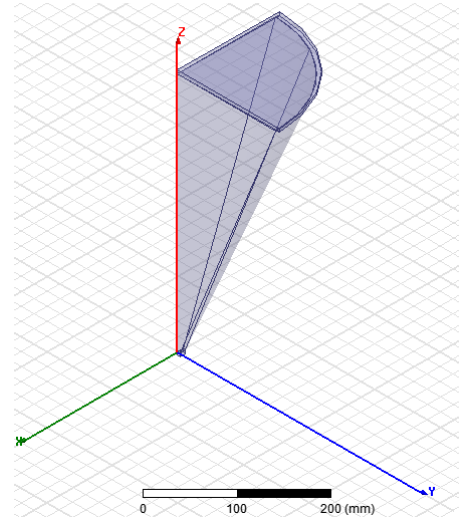


Fig. 3. Showing the HFSS simulation set up of the conical horn and the simulated fields inside.

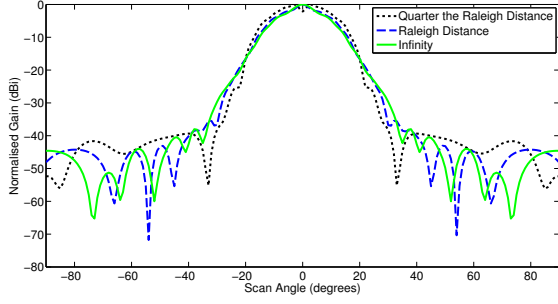


Fig. 4. Normalised simulated fields at 1.25m, 2.25m and infinity from a conical horn with the same aperture size as the AUT.

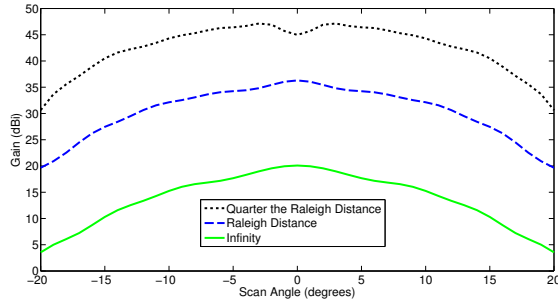


Fig. 5. Simulated fields at 1.25m, 2.25m and infinity from a conical horn with the same aperture size as the AUT.

$$d = \sqrt{3 \lambda L_S} \quad (2)$$

The fields inside the horn can be seen in figure 3. The external fields of this horn were sampled at the following distances:

- Quarter the Raleigh Distance = 0.56 m
- The Raleigh Distance = 2.25 m
- True far-field = infinity

The normalised pattern results are shown in figure 4. It can be seen that the ideal patterns are shown by the true far-field, and distances smaller than that as calculated by the Raleigh Distance show significant disturbance. Figure 5 shows the gain of the pattern sampled at different distances and how the measurements in the near field over estimate the gain of the antenna by 27dBi. This is because these disturbed measurements are being taken in the near field. Therefore to correctly measure an antenna the walls of the chamber must be further away from the AUT than the Raleigh Distance, this is in line with current practice described earlier.

IV. CALIBRATION OF LOSSES IN AN ANECHOIC CHAMBER

When an anechoic chamber is used to measure the absolute gain of an AUT, the losses through the chamber need to be measured and characterised so that they can be calibrated out of the measurement. This

includes all cable, connection, instrumentation and free space losses.

To directly measure the gain of an AUT, it is usual practice to compare the AUT to the measurement of a SGH of known and calibrated gain, equation 3 [13], as derived from the Friis equation [14]. Where G_T (dB) is the gain of the AUT, G_S (dB) is the known Gain of the SGH, P_T (W) is the power received by the AUT and P_S (W) is the power received by the SGH when measured on the range.

$$(G_T)_{dB} = (G_S)_{dB} + 10 \log_{10} \frac{P_T}{P_S} \quad (3)$$

Ideally, this involves taking measurements of the antenna and the SGH at the same time and with the same experimental set up. In reality, the measurements have to be taken sequentially and the losses of the additional hardware taken into account in the calculation. This accounts for any variations in the range with time and ensures these are not attributed to the antenna behaviour. The measurement is typically taken as a function of frequency and calculated using amplitudes only. The SGH should be illuminated by a plane wave of the same polarisation as the AUT.

The measurement of the SGH on the range, P_S , gives the calibration of the range by measuring the losses through the range. The chamber losses should be measured by using a calibrated SGH that has been tested and characterised using an outdoor range.

If it is not possible to use a calibrated SGH then the gain of a SGH can be estimated from its collecting area as a function of frequency, as shown in equation 4. Here G (dB) is the calculated gain of the antenna, A_P (m^2) is the physical area of the antenna and η_a (%) is the aperture efficiency of the antenna type in question. The aperture efficiency describes how efficient the antenna is at absorbing or emitting incoming plane waves at the wavelength in question and is a general term that includes aperture illumination efficiency, spill over losses, phase-error, blockage, depolarisation.

$$G_{dB} = 10 \log_{10} \left(4 \pi \frac{A_P}{\lambda^2} \eta_a \right) \quad (4)$$

For example, from equation 4, the gain of a SGH with an aperture of 54 x 74 mm at 15 GHz with an aperture efficiency of 70% is calculated to be 19.44 dBi. The difference between the calculated and calibrated performance of this SGH as a function of frequency can be seen in figure 6. This shows that using the calculated values will introduce small errors at some frequencies, so the manufacturers calibrated values should be used if at all possible.

In addition, Figure 6 shows that there is a trend of increasing in gain as frequency increases, as demon-

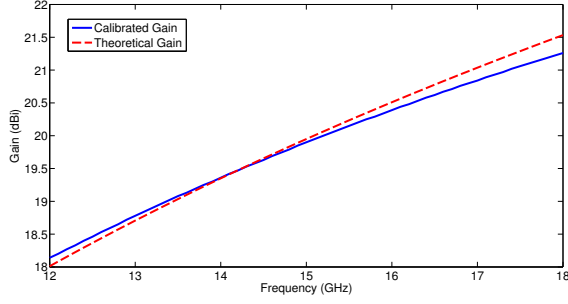


Fig. 6. Showing the calibrated and calculated performance for the standard gain horn antenna.

strated by Equations 4 and 5 [15]. Where v (ms^{-1}) is the velocity and f (Hz) is the frequency of the electromagnetic wave in question.

$$v = f \lambda \quad (5)$$

This calibration process is suitable for a single channel AUT. If a multi-channel AUT is to be measured then the RF path for each channel must be individually measured and calibrated. This is because the RF path for each channel will be unique as the measurement of a multi-channel AUT requires the addition of a multiplexer and additional cables to enable the measurement of multiple channels. In addition measurements should be taken in magnitude and phase.

V. EQUATIONS TO CALIBRATE AN ANECHOIC CHAMBER FOR MULTI-CHANNEL AUT MEASUREMENT

To complete a true measurement of losses in an anechoic chamber for a multi-channel AUT, all measurements should be vectors and calculations completed as phasors. The measurement of a SGH, (SGH_M) as a complex gain in dimensionless units relative to an isotropic radiator, allows a range calibration and the gain of the AUT to be calculated. This measurement quantifies the losses through the range (L_R) if the calibrated gain of the SGH is known (SGH_C (dB)) and the additional hardware losses for the SGH are measured (L_{SGH}), as shown in equation 6. The additional hardware should be added at a matched plane so reflection losses can be ignored. If this is not possible then it is possible to use isolators or attenuators at either side of the split plane to achieve this result. It should be remembered that all losses have a negative value and all gains a positive value.

$$SGH_M = \frac{10^{\frac{SGH_C}{10}}}{L_{SGH}} L_R \quad (6)$$

Once this calibration is completed the SGH can be swapped for the AUT and its performance measured in

the anechoic chamber (AUT_M). The additional hardware set-up losses for the AUT should be measured (L_{AUT}). From these values the gain and phase of the AUT (AUT_G (dB)) can be calculated as shown in equation 7.

$$AUT_G = 10 \log_{10} \frac{|AUT_M| |L_{AUT}|}{|L_R|} \quad (7)$$

Equations 6 and 7 can be combined as shown in equation 8 to directly calculate the gain of an AUT measured in an anechoic chamber by comparison to a SGH.

$$AUT_G = 10 \log_{10} \frac{|AUT_M| |L_{AUT}| 10^{\frac{SGH_C}{10}}}{|SGH_M| |L_{SGH}|} \quad (8)$$

Since a multi-channel AUT is being measured this calibration process needs to be repeated for the RF path for each channel to be measured and will be presented in the next section.

VI. ANECHOIC CHAMBER CALIBRATION FOR A MULTI-CHANNEL AUT

The following calibration is for the anechoic chamber and positioning system described in this paper. If the process is adapted it will be applicable to any anechoic chamber.

A SGH, whose calibration can be seen in figure 6, was mounted in the positioner and a measurement taken for each of the four RF paths. This gives the SGH_M for each of the individual channels. These results are shown in figure 7. It can be seen that each path is unique; in this particular case this is due to the use of a multiplexer and short hand-formable semi-rigid coax cables to connect the AUT to the measurement path. Therefore, to avoid errors, it is important that each channel is calibrated individually.

In addition to the losses through the RF measurement path, additional hardware is required to connect the SGH to the measurement system. This additional hardware is a cable, its loss measured as a function of frequency is L_{SGH} and is shown in figure 8. In this case the additional hardware occurs in the common RF path for each channel, a single measurement can be used for all channels.

Next the SGH is replaced with the AUT measurement repeated through each RF channel, giving AUT_M , as shown in figure 9. It can be seen that each channel performs differently as a function of frequency. This is in part due to the different hardware path for each channel and in part inherent with the monopulse antenna.

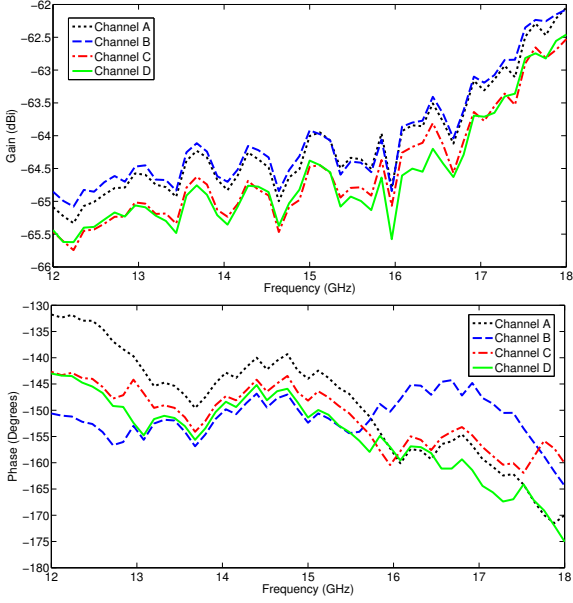


Fig. 7. The SGH_M for the 4 RF paths measured in the anechoic chamber.

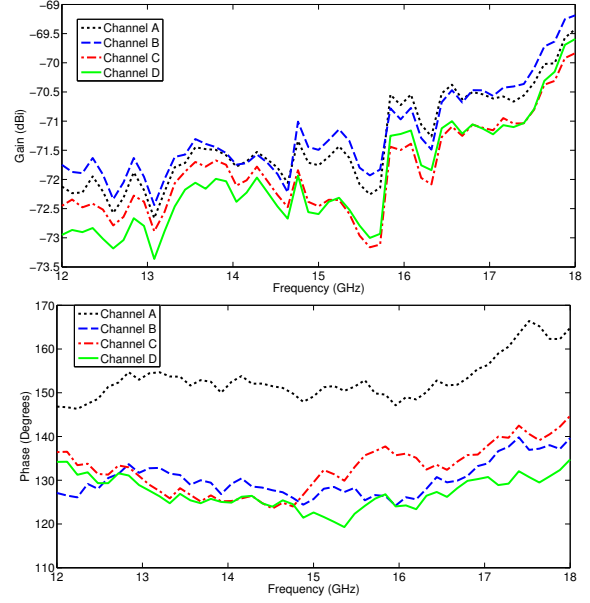


Fig. 9. The AUT_M for the 4 RF paths measured in the anechoic chamber.

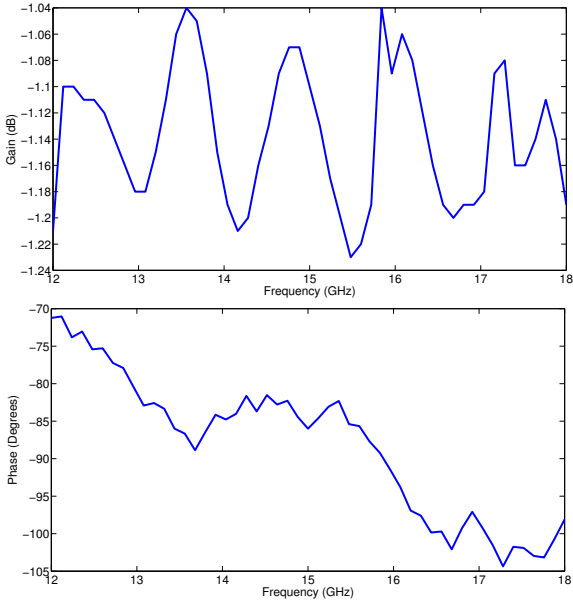


Fig. 8. The L_{SGH} for the additional cable required to test the SGH in the anechoic chamber.

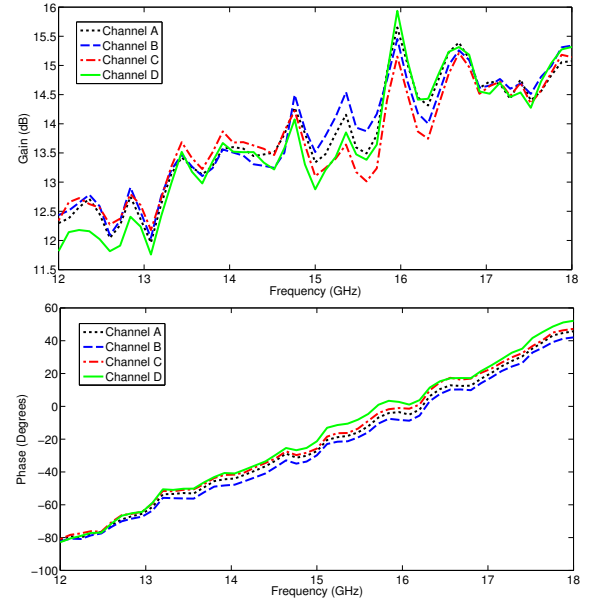


Fig. 10. The AUT_G as calibrated for a multi-channel antenna.

When these results are combined as shown in equation 8 the AUT_G for each channel of the antenna can be plotted as shown in figure 10.

As can be seen, the four different channels of the multi-channel antenna inherently perform differently as a function of frequency. If a single calibration had been applied to all channels this variation would still be present, but there would be an additional difference due to the hardware set up that was not accounted for. Calculations should be completed at phasors as the phase varies between channels and this difference needs to be accounted for to remove additional sources

of error. Highlighted is the importance of calibrating each of the four RF paths individually, not using just a single calibration, and that the calculations should be performed as phasors. These four channels can be combined together using a comparator to calculate the true gain of the multi-channel AUT.

VII. CONCLUSIONS

This paper has described the procedure to calibrate a multi-channel AUT in an anechoic chamber. This is a novel extension to current practice that describes the calibration of an anechoic chamber for a single channel antenna. It presents the best practice that

the RF path for each of the channels is measured separately, recording both magnitude and phase. All calculations presented should be conducted as phasors. It can be seen that the calibrated antenna gain gives the true gain of the antenna and does not suffer from the range effects that would give false readings. This calibration process can be applied to many different types of measurement ranges.

REFERENCES

- [1] W. H. Emerson, "Anechoic chamber," Patent US 3 308 463, 03 07, 1967.
- [2] W. H. Emerson, "Emerson anechoic chamber," Patent US 3 273 150, 09 13, 1966.
- [3] B. K. Chung and H. T. Chuah, "Advice on limiting exposure to electromagnetic fields (0-300GHz)," *National Radiological Protection Board*, vol. 15, 2004.
- [4] B. K. Chung and H. T. Chuah, "Modeling of rf absorber for application in the design of anechoic chamber technologies for future precision strike missile systems," *Progress In Electromagnetics Research*, vol. 43, pp. 273–285, 2003.
- [5] M. Gillette, "Rf anechoic chamber design using ray tracing," in *Antennas and Propagation Society International Symposium, 1977*, vol. 15, 1977, pp. 246–249.
- [6] T. L. Sheret and B. Allen, "Axis transform to characterise a monopulse twist reflector antenna and radome in an anechoic chamber," in *Loughborough Antenna and Propagation Conference*, 2014.
- [7] M. Barron, "Specifying and procuring a 10 meter semi-anechoic emc chamber," in *Electromagnetic Compatibility, 2000. IEEE International Symposium on*, vol. 1, 2000, pp. 231–236 vol.1.
- [8] Institute of Electrical and Electronics Engineers. Antenna Standards Committee, *IEEE standard test procedures for antennas*, ser. Ieee Std 149-1979 Series. Institute of Electrical and Electronics Engineers : distributed in cooperation with Wiley-Interscience, 1979.
- [9] A. Yaghjian, "An overview of near-field antenna measurements," *Antennas and Propagation, IEEE Transactions on*, vol. 34, no. 1, pp. 30–45, Jan 1986.
- [10] EMSCAN Corporation, *RFxpert Training Manual*, 2012. [Online]. Available: http://www.emcan.com/downloads/RFxpert/Technical_Resources/RFxpert_Training_Manual.pdf
- [11] D. Y. Huang and K. Boyle, *Antennas: From Theory to Practice*. Wiley, 2008.
- [12] T. Teshirogi and T. Yoneyama, *Modern Millimeter-wave Technologies*, ser. Wave Summit Series. Ohmsha, 2001.
- [13] "Ieee standard test procedures for antennas," *ANSI/IEEE Std 149-1979*, 1979.
- [14] A. Rudge, *The Handbook of antenna design*, ser. IEE electromagnetic waves series. P. Peregrinus on behalf of the Institution of Electrical Engineers, 1983, no. v. 2.
- [15] F. Keller, W. Gettys, and M. Skove, *Physics, classical and modern*. McGraw-Hill, 1993.